APPENDIX A

RADIO PROPAGATION PATH DELAYS

To accomplish time transfer via radio waves, the radio propagation path delay has to be determined as accurately as possible. If microsecond or sub-microsecond accuracies are required then the path delay must be determined by a portable clock trip. If only millisecond accuracies are required, then calculations can be accomplished of the Great Circle distance and the associated propagation path delay.

COMPUTATION OF THE GREAT CIRCLE DISTANCE

With the advent of hand-held scientific calculators such as the HP-21 or HP-25 calculators, the Great Circle distance can be quickly calculated provided the latitude and longitude of both the transmitter and receiver are known.

$$D = \cos^{-1} [\sin(lat_A) * \sin(lat_B) + \cos(lat_A) * \cos(lat_B) * \cos(lng_B \pm lng_A)] * 60$$

Where D = Great Circle distance in nautical miles and sign between lng is + if A and B are not on same side of Equator.

Example:
What is the Great Circle distance between WWV (Ft. Collins, Colorado) and Palo Alto, California.

$$
\begin{aligned}
\text{WWV} \quad & \text{Latitude} = Lat_A = 40°41' = 40.68333\ldots° \\
& \text{Longitude} = Lng_A = 105°02' = 105.0333\ldots° \\
\text{Palo Alto} \quad & \text{Latitude} = Lat_B = 37°23' = 37.38333\ldots° \\
& \text{Longitude} = Lng_B = 122°09' = 120.15° \\
Lng_B - Lng_A \quad & = 122°09' - 105°02' = 17.1166667°
\end{aligned}
$$

$$D = \cos^{-1} [\sin(lat_A) * \sin(lat_B) + \cos(lat_A) * \cos(lat_B) * \cos(lng_B - lng_A)] * 60$$

using the HP-21

$$
\begin{aligned}
D &= 820.4908374 \text{ nautical miles} \\
&= 1519.549 \text{ km}
\end{aligned}
$$

TRANSMISSION MODES

The ground-wave propagation path (most LF transmissions under 1000 km and HF transmissions under 100 km) closely follows the Great Circle route between the transmitter and receiver. However, HF transmissions over a distance of more than about 160 kilometers follow sky-wave paths. VLF transmissions from distances over 1000 km are almost pure skywaves; but for shorter ranges the received signals are a varying mixture of several paths. VLF skywaves are reflected from the D layer at heights of 70 km daytime and 90 km at night. LF skywaves are reflected from the E layer.

HF SIGNAL MULTIPLE HOPS

The maximum distance that can be spanned by a single hop (i.e. one reflection from the iono-sphere) via the F2 layer is about 4000 km (Figure A-1). Therefore, the fewest number of hops be-tween transmitter and receiver is the next integer greater than the Great Circle distance (in kilometers) divided by 4000. Transmission modes with one or two more hops than the minimum number of hops occur frequently (Figure A-3), but modes of higher order are greatly attenuated during transmission and are of little concern.
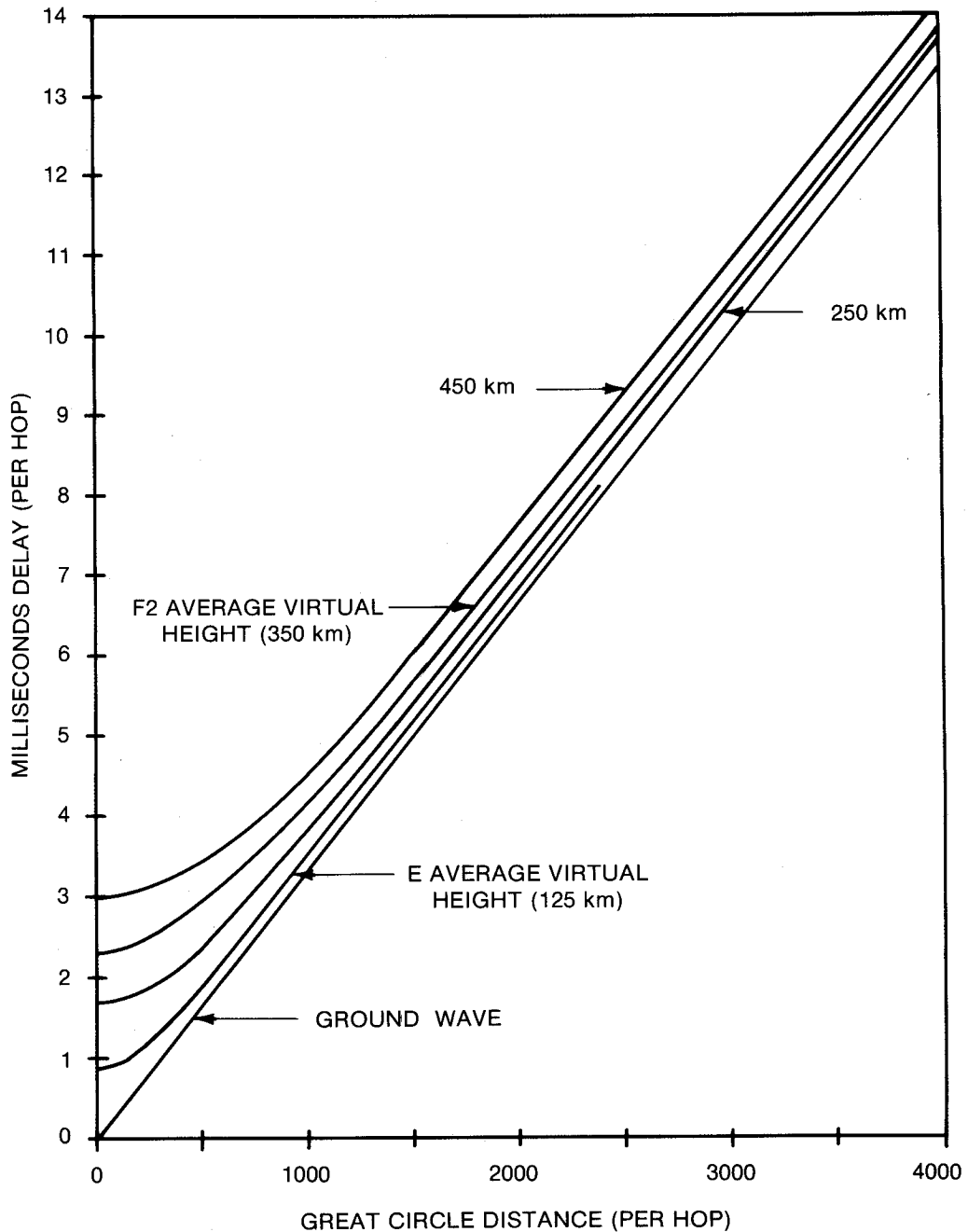

Figure A-1. Transmission Delay Graph

Example 1: Find the minimum number of hops for a distance of 3923 km.
Solution: A one-hop F2 mode is possible (3923 ÷ 4000 <1).
Example 2: What modes are likely to be received at a distance of 7687 km?
Solution: Two-hop, three-hop, and four-hop F2 modes can be expected (7687 ÷ 4000 >1,
             but <2).

Useful transmissions via the E layer (daytime only) are usually limited to one-hop modes up to a distance of about 2400 km.

Remember that some locations may receive transmissions from both the E and F2 layers and that transmissions may be reflected occassionally from layers other than E and F2.

The following approach should improve your estimate of propagation delay:

Determine which modes are possible at your location.

Tune to the highest frequency which provides consistent reception to reduce interference from high-order modes.

If several modes are being received (indicated by multiple tick reception or tick jitter between fairly constant positions), select the tick with earliest arrival time for measurements.

After plotting time measurements for several weeks, either disregard measurements which are conspicuously out of place, or correct measurement to the more likely mode if the plot is mistimed by the difference in time between possible modes.
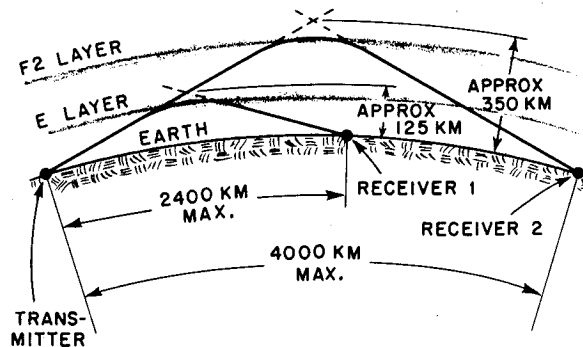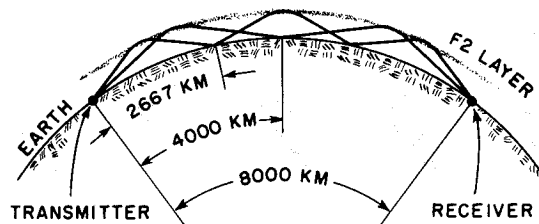

Figure A-2. Single-hop Sky-wave Paths

Figure A-3. Multiple-hop Transmission Path

A-3

HEIGHT OF IONOSPHERE

Long-distance HF transmissions are usually reflected from the F2 layer, which varies in height from about 250 to 450 km. Experience has shown that the virtual height of the F2 layer averages about 350 km (Figure A-2). Unless special studies permit determination of layer height, 350 km can be used for delay estimation.

The E layer is dense enough to reflect HF transmissions only during the daytime at a virtual height of about 125 km (Figure A-2). One hop E modes may provide very steady daytime reception at distances up to about 2400 km.

DELAY DETERMINATION

Once the transmitter-to-receiver distance, possible transmission modes, and layer heights have been determined, transmission delay can be found graphically from Figure A-1. The shaded area along the F2 curve shows the possible extremes of height variation.

As shown in the following examples, the delay for a one-hop mode can be read directly from the transmission delay graph for a given distance and layer height.

Example 1: Find the one-hop delay for a distance of 3923 km.
Solution: Expected F2 delay is about 13.60 ms. No one-hop E mode is likely since the distance is greater than the usual limit of 2400 km for the one-hop E mode.

Example 2: Find the one-hop delay for a distance of 2200 km.
Solution: Expected F2 delay is about 7.90 ms; expected E delay is about 7.50 ms.

For a multi-hop mode:
a) Determine the distance covered by each hop.
b) Find the delay for a single hop.
c) Multiply the single-hop delay by the number of hops to determine the total delay.

Example 3: Find the two-hop delay for a distance of 3923 km.
Solution: Each 1962 km hop contributes a delay of about 7.15 ms, the total delay is 7.15 x 2 or 14.30 ms. Note that the two-hop delay for a 3923 km distance is 0.7 ms greater than the one-hop delay for the same distance determined in Example 1 above.

Example 4: Find the three-hop delay for a distance of 7687 km.
Solution: The delay contributed by each 2562 km hop is about 9.05 ms; the total delay is is 9.05 x 3 or 27.15 ms.

Example 5: Find the four-hop delay for a distance of 7687 km.
Solution: The delay contributed by each 1922-km hop is about 6.95 ms; the total delay is 6.95 x 4 or 27.80 ms. Note that the four-hop delay for 7687-km distance is 0.65 ms greater than the three-hop delay for the same distance determined in example above.
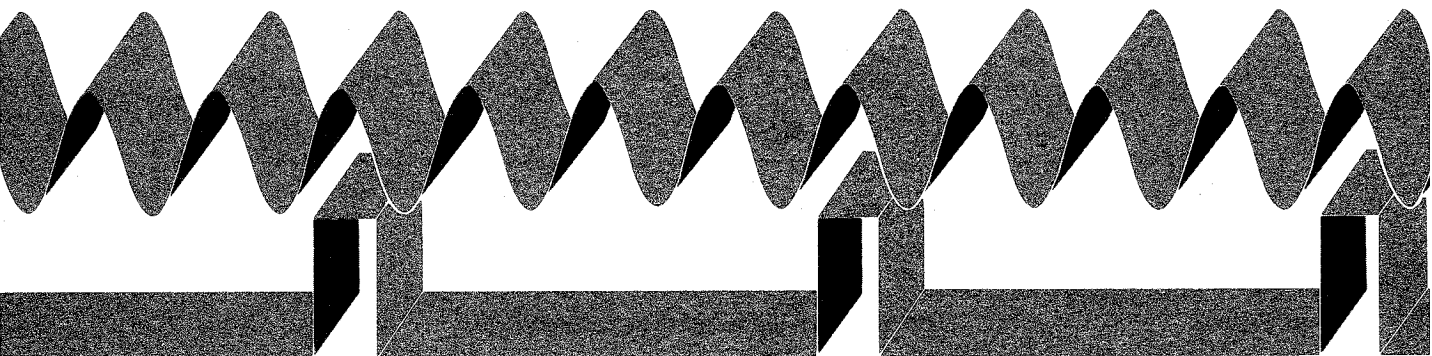
APPENDIX B

DERIVATION OF TIME ERROR EQUATION

As mentioned in Section II, the frequency at any time t can be expressed (with the rate of frequency shift approximately by a straight line):
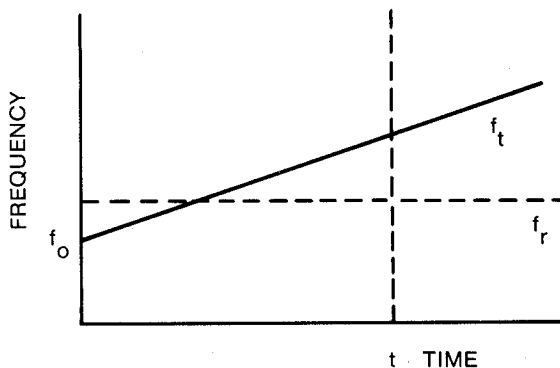
$$f_t = f_o + af_r t \qquad \text{(Eq. 1)}$$

Figure B-1. Oscillator Frequency Vs. Time

where: f_t = frequency at time t
f_o = initial frequency at time t = o
f_r = reference frequency (standard)
a = aging rate or drift

Aging rate or drift rate is the fractional rate of change of frequency per unit of time. The aging rate or drift is generally stated in terms of fractional frequency deviation per unit of time. Fractional frequency deviation is defined as:

$$\frac{\Delta f}{f_r} = \frac{f_2 - f_1}{f_r}$$

$$f_1 = f_t \text{ at } t_1$$
$$f_2 = f_t \text{ at } t_2$$

For quartz oscillators the aging rate is normally stated in terms of daily fractional frequency deviation; e.g., $\pm 5 \times 10^{-10}$/day. Whereas the drift (rather than aging rate) of rubidium standards is specified on a per month basis; e.g., $\pm 1 \times 10^{-11}$/month.

Now, since f_t differs by a small amount from f_r, the clock, based upon this oscillator, will gain or lose time because each oscillator cycle is a little short or long. In the case illustrated by the sketch, f_t is increasing with respect to f_r; the time of each cycle the oscillator makes is short by an amount L.

$$L = \frac{1}{f_r} - \frac{1}{f_t}$$

B-1

In an arbitrarily short time Δt, there are $f_t \Delta t$ cycles. The incremental time error ΔE can be written:

$$\Delta E = L f_t \Delta t$$

$$= \left(\frac{1}{f_r} - \frac{1}{f_t} \right) f_t \, \Delta t$$

Taken to the limit,

$$dE = \left(\frac{1}{f_r} - \frac{1}{f_t} \right) f_t dt = \left(\frac{f_t}{f_r} - 1 \right) dt$$

To obtain E,

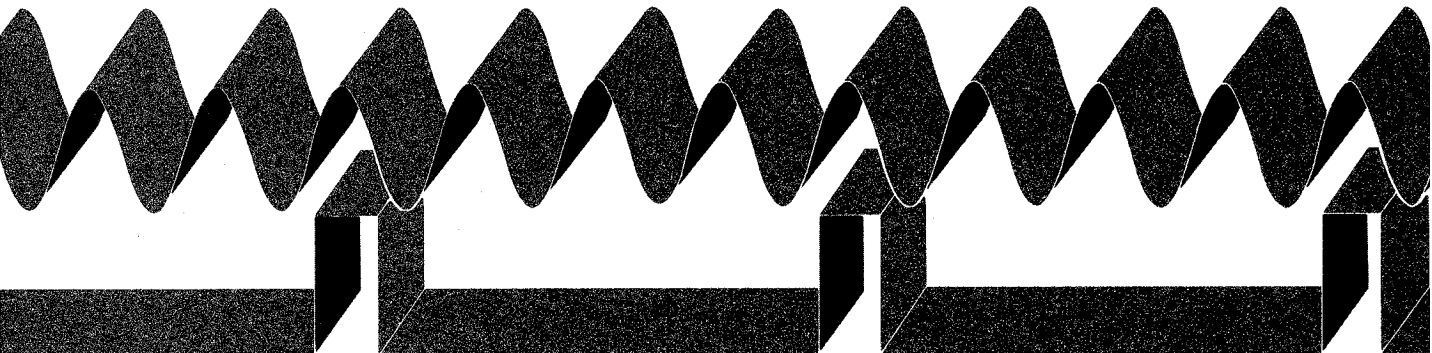$$E = \int \frac{f_t}{f_r} \, dt - \int dt$$

But:

$$f_t = f_o + a f_r t$$

Therefore:

$$E = \int \frac{f_o + a f_r t}{f_r} \, dt - \int dt = \int \frac{f_o}{f_r} \, dt + \int at \, dt - \int dt$$

$$E = \frac{f_o}{f_r} t + \frac{at^2}{2} - t + c$$

At $t = o$, $c = E_o$, the initial error. Therefore the total time error is:

$$E = E_o + \left(\frac{f_o}{f_r} - 1 \right) t + \frac{at^2}{2} \qquad \text{(Eq. 2)}$$

APPENDIX C

RECALIBRATION CHARTS FOR QUARTZ
OSCILLATORS AND RUBIDIUM STANDARDS

Figures C-1 and C-2 are useful for estimating the length in days of the recalibration cycle for an oscillator with known drift rate to keep the time system based on it within prescribed error limits. A recalibration cycle is the time, in days, that can be allowed to pass between calibration adjustments. A shorter cycle (more frequent adjustments) is needed to keep a system accurate to $\pm100\mu s$ (total time excursion, $2E_O = 200\mu s$) than to, say, 1 ms.

To use the charts, select the slant line marked for the aging or drift rate (in parts per day for quartz oscillators and parts per month for rubidium standards) of the oscillator. Note the intersection of this line with the horizontal line corresponding to the permitted error excursion. This intersection, referred down to the horizontal axis, gives the recalibration cycle.

Example:
A time system is to be maintained to within 10 ms based on a quartz oscillator with a positive aging rate, $a = 5\times10^{-10}$/day. To use the chart to estimate the length of the recalibration cycle, locate the slant line marked "5×10^{-10}/day" and note its intersection with the horizontal line corresponding to a total time excursion of 20 ms (±10 ms). The answer read from the chart is 60 days (computed answer using the formulae in Section II is 60.8 days). Note that to use Figure C-1, aging rate must be expressed in parts/day and permitted time excursion, in milliseconds.

Example:
A rubidium based time system is to be maintained within $10\mu s$. The drift rate is a positive 1×10^{-11}/month. Looking at the appropriate slant line corresponding to the drift rate yields a recalibration time of 101 days for $2E_O = 20\mu s$.

These charts provide graphical solutions to the equation:

$$T_2 = 4\sqrt{\frac{E_O}{a}}$$

where:
  T_2 = number of days between oscillator recalibrations
  E_O = error limit, ms or μs
  a = drift rate, parts/day or parts/month

To obtain a straight-line plot, this equation is placed in slope-intercept form ($y = mx + b$):

$$T_2 = 4\sqrt{\frac{E_O}{a}}$$

$$T_2^2 = 16\frac{E_O}{a} = \frac{8}{a}(2E_O)$$

$$2E_O = \left(\frac{a}{8}\right)T_2^2$$

$$\log(2E_O) = 2\log T_2 + \log\frac{a}{8}$$

The log-log plot is a line with slope = 2 and intercept = $\log\frac{a}{8}$. For selected values of "a",

Figure C-1 and C-2 show the regions of interest.
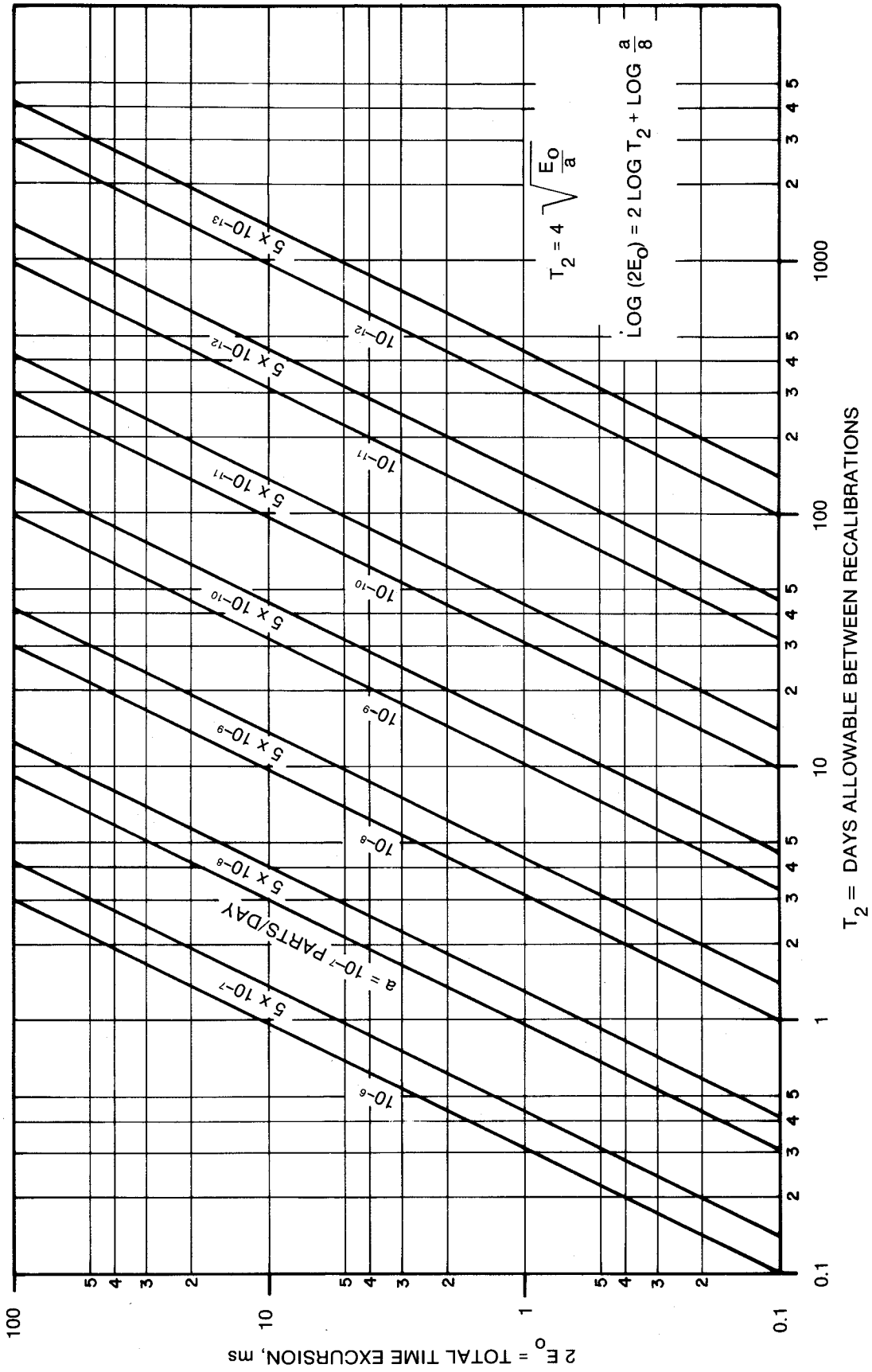
Figure C-1. Recalibration Chart for Quartz Oscillators

$$T_2 = 4 \sqrt{\frac{E_O}{a}}$$

$$\text{LOG} (2E_O) = 2 \text{ LOG } T_2 + \text{LOG } \frac{a}{8}$$

$T_2 = $ DAYS ALLOWABLE BETWEEN RECALIBRATIONS

$2 E_O = $ TOTAL TIME EXCURSION, ms
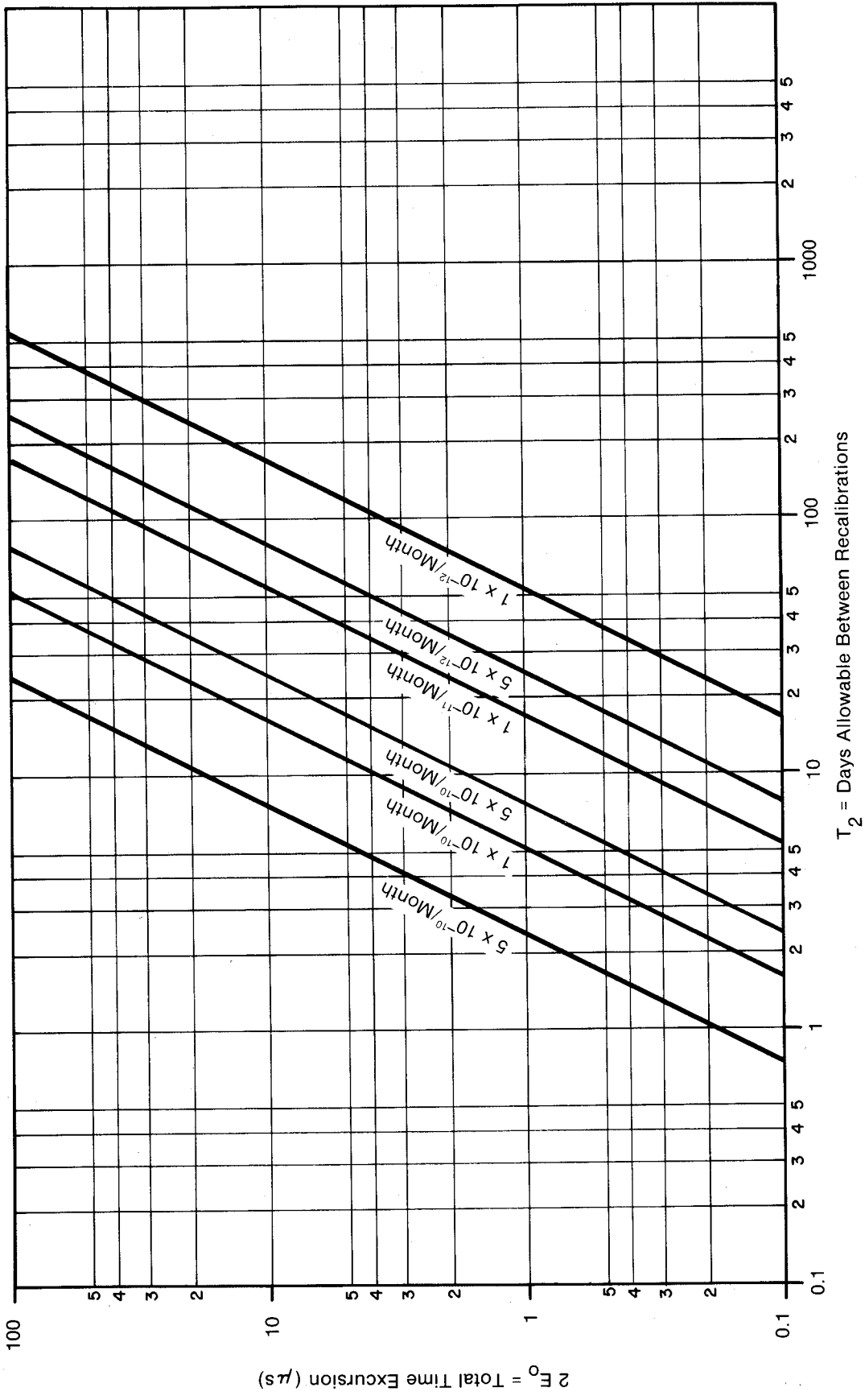
Figure C-2. Recalibration Chart for Rubidium Standards

The chart axes and labels:

- Horizontal axis: T_2 = Days Allowable Between Recalibrations
- Vertical axis: $2 E_o$ = Total Time Excursion (μs)

Line labels:
- 1×10^{-12}/Month
- 5×10^{-12}/Month
- 1×10^{-11}/Month
- 5×10^{-10}/Month
- 1×10^{-10}/Month
- 5×10^{-10}/Month

To calculate the oscillator's frequency offset f_O, it is necessary to know T_1. This value is easily computed from the value of T_2, which has been read from the chart for the first example:

$$T_1 = \frac{T_2}{2} = \frac{60}{2} = 30 \text{ days}$$

$$f_O = f_r (1 - aT_1) = f_r \left[1 - (5 \times 10^{-10}) (30)\right]$$
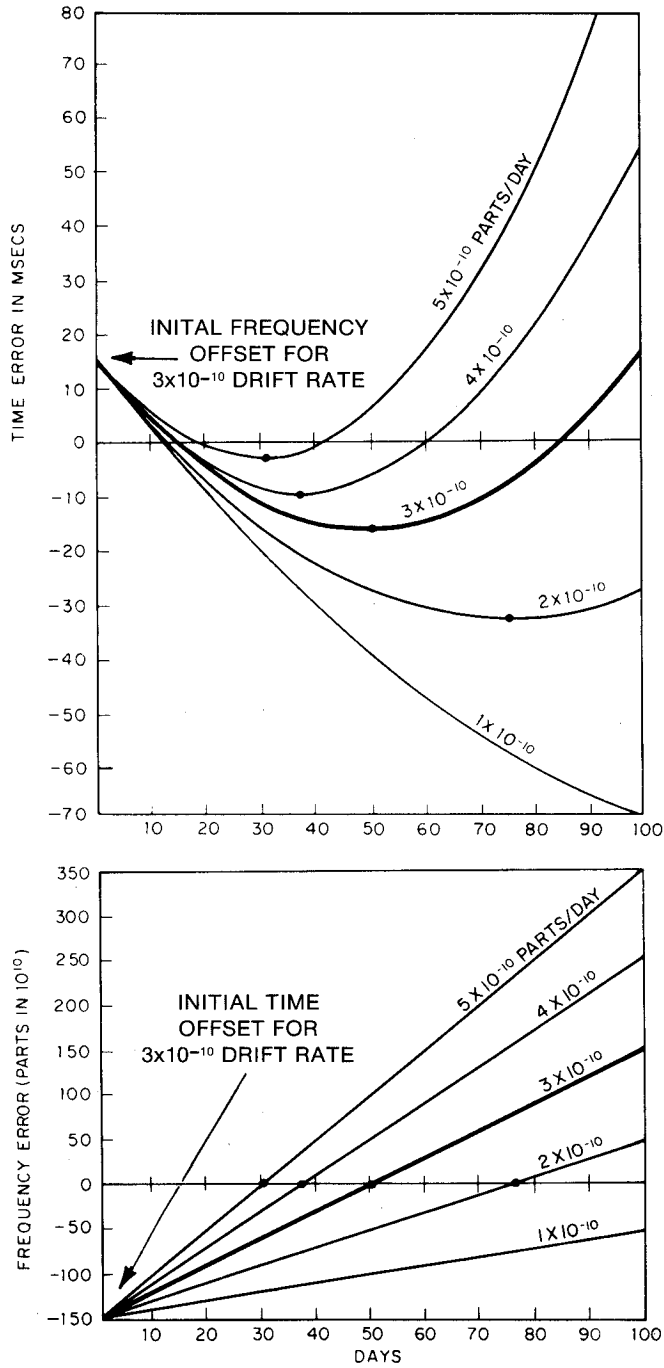
$$= f_r \left[(1 - 150 \times 10^{-10})\right]$$

Figure C-3. Error Plots

C-4

Frequency offset is, then –150 parts in 10^{10}.

DRIFT RATE PREDICTION

It should be recognized that unless the drift rate actually is the one predicted for the oscillator, use of this method may enlarge rather than minimize error. Figure C-3 shows this effect.

In a typical case, frequency drift was assumed to be 3×10^{-10}, parts per day (heavy solid line); the initial frequency was offset –150 parts in 10^{10} and the initial time was offset 16 ms to minimize error over a 100-day period. The plots of Figure C-3 show the increased time error that would result if oscillator performance were at a drift rate other than the 3 parts in 10^{10} predicted say, at 1, 2, 4 or 5 parts in 10^{10}.

Caution should be exercised in using the derived recalibration times. The equations, as well as the charts, are based on constant conditions, e.g. temperature, humidity etc. Changing conditions can cause frequency changes which will impact on accumulated time.

APPENDIX D
VARIANCE OF TIME INTERVAL
FOR CALIBRATED CLOCKS*

We assume a calibration time interval, T_c, during which the system clock is compared against a reference to determine its average frequency. Following a dead time, T_d, the phase or time of the clock is measured and we wish to estimate the variance in the indicated time after an interval T_p where we assume the correction determined during the calibration is applied.
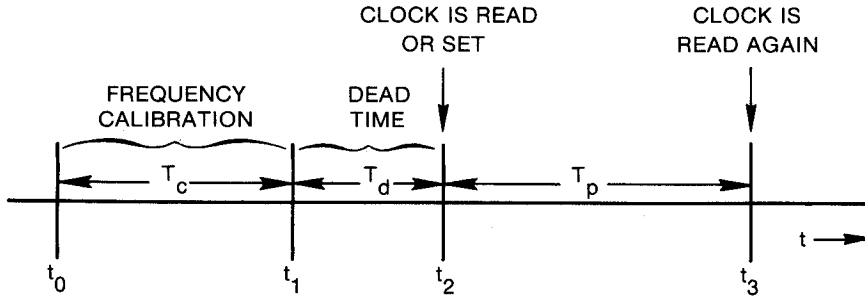
The frequency offset determined during the calibration interval is

$$\frac{\Delta f_c}{f_0} = \frac{\phi(t_1) - \phi(t_0)}{\omega_0 T_c} \qquad \text{(Eq. 1)}$$

$$\omega_0 = 2\pi f_0$$

where the reference clock is assumed to have output voltage

$$v_r = V_0 \cos \omega_0 t$$

and the system clock has

$$v_s = V_0 \cos [\omega_0 t + \phi(t)]$$

The time error, ϵ, developed during the time, T_p, after applying the correction factor is then just

$$\epsilon = T_p \left(\frac{\Delta f_p}{f_0} - \frac{\Delta f_c}{f_0} \right) \qquad \text{(Eq. 2)}$$

where

$$\frac{\Delta f_p}{f_0} = \frac{\phi(t_3) - \phi(t_2)}{\omega_0 T_p}$$

---

*Extracted from an unpublished paper, same title, by Dr. Len Cutler of Hewlett-Packard Laboratories, undated.

so that

$$\epsilon = \frac{T_p}{\omega_0} \left(\frac{\phi_3 - \phi_2}{T_p} - \frac{\phi_1 - \phi_0}{T_c} \right)$$

or

$$= \frac{1}{\omega_0} \left(\phi_3 - \phi_2 - (\phi_1 - \phi_0) \frac{T_p}{T_c} \right)$$

Now

$$\overline{\epsilon} = \frac{1}{\omega_0} \left(\overline{\phi_3} - \overline{\phi_2} - (\overline{\phi_1} - \overline{\phi_0}) \frac{T_p}{T_c} \right) = 0$$

and

$$\overline{\epsilon^2} = \frac{1}{\omega_0^2} \left[\overline{\phi_3^2} + \overline{\phi_2^2} + \frac{T_p^2}{T_c^2} \left(\overline{\phi_1^2} + \overline{\phi_0^2} \right) \right.$$

$$- 2\overline{\phi_3\phi_2} - \frac{2T_p}{T_c} \overline{\phi_3\phi_1} + \frac{2T_p}{T_c} \overline{\phi_3\phi_0}$$

$$\left. + \frac{2T_p}{T_c} \overline{(\phi_2\phi_1)} - \frac{2T_p}{T_c} \overline{\phi_2\phi_0} - 2\overline{\phi_1\phi_0} \frac{T_p^2}{T_c^2} \right]$$

ϵ is a stationary, Gaussian distributed random variable. Even though the phase is not stationary, we can say, using the autocorrelation function, $R(\tau)$:

$$\overline{\epsilon^2} = \frac{2}{\omega_0^2} \left[R_\phi(0) \left(1 + \frac{T_p^2}{T_c^2} \right) - R_\phi(T_p) - \frac{T_p}{T_c} R_\phi(T_p + T_d) \right.$$

$$+ \frac{T_p}{T_c} R_\phi(T_p + T_d + T_c) + \frac{T_p}{T_c} R_\phi(T_d) - \frac{T_p}{T_c} R_\phi(T_c + T_d)$$

$$\left. - \frac{T_p^2}{T_c^2} R_\phi(T_c) \right]$$

Then

$$\overline{\epsilon^2} = \frac{2}{\omega_0^2} \int_0^\infty df\, S_\phi(f) \left[1 + \frac{T_p^2}{T_c^2} - \cos 2\pi f\, T_p \right.$$

$$- \frac{T_p}{T_c} \cos 2\pi f\, (T_p + T_d) + \frac{T_p}{T_c} \cos 2\pi f (T_p + T_d + T_c)$$

$$+ \frac{T_p}{T_c} \cos 2\pi f\, T_d - \frac{T_p}{T_c} \cos 2\pi f (T_c + T_d)$$

$$\left. - \frac{T_p^2}{T_c^2} \cos 2\pi f\, T_c \right] \qquad\qquad \text{(Eq. 3)}$$

or

$$\overline{\epsilon^2} = \frac{2}{\omega_0^2} \int_0^\infty df\, S_\phi(f)\, K(f, T),$$

since

$$R_\phi(\tau) = \int_0^\infty S_\phi(f)\, \cos 2\pi f\tau\, df ,$$

where $S_\phi(f)$ is the one-sided spectral density of phase.

Let

$$S_y(f) = A + \frac{B}{f} \qquad\qquad \text{(Eq. 4)}$$

where

$$S_y(f) = \frac{S_\phi(f)}{\omega_0^2} = \frac{f^2 S_\phi(f)}{f_0^2}$$

$S_y(f)$ is the fractional frequency spectral density. The phase spectral density is then

$$S_\phi(f) = \frac{f_0^2}{f^2}\, S_y(f)$$

Using Equation (4) in Equation (3), we get

white frequency

flicker frequency

$$\overline{\epsilon^2} = \frac{2}{4\pi^2} \int_0^\infty df \left(\frac{A}{f^2} + \frac{B}{f^3} \right) K(f, T) ,$$

D-3

where K(f,T) is defined in Equation (3). The white part gives

$$\overline{\epsilon_w^2} = \frac{1}{2} A \left(T_p + \frac{T_p^2}{T_c}\right) \quad = \frac{1}{2} A T_p \left(1 + \frac{T_p}{T_c}\right)$$

(Eq. 5)

The flicker part gives

$$\overline{\epsilon_f^2} = B T_p^2 \left[\frac{(T_p + T_d + T_c)^2}{T_p T_c} \ln\left(1 + \frac{T_p + T_d}{T_c}\right) + \frac{T_d^2}{T_c T_p} \ln \frac{T_d}{T_c} \right.$$

$$- \ln \frac{T_p}{T_c} \quad - \frac{(T_p + T_d)^2}{T_p T_c} \ln\left(\frac{T_p + T_d}{T_c}\right)$$

$$\left. - \frac{(T_c + T_d)^2}{T_p T_c} \ln\left(1 + \frac{T_d}{T_c}\right) \right]$$

(Eq. 6)

Typical values for A and B are

	5061A	5061A Opt. 004
A	$\approx 1 \times 10^{-20}$ sec	1.28×10^{-22} sec
B	$\approx 2.88 \times 10^{-26}$	6.5×10^{-28}

The value for A is that at the end of beam tube life and that for B is an estimate of what one might expect for a typical non-controlled laboratory type of environment.
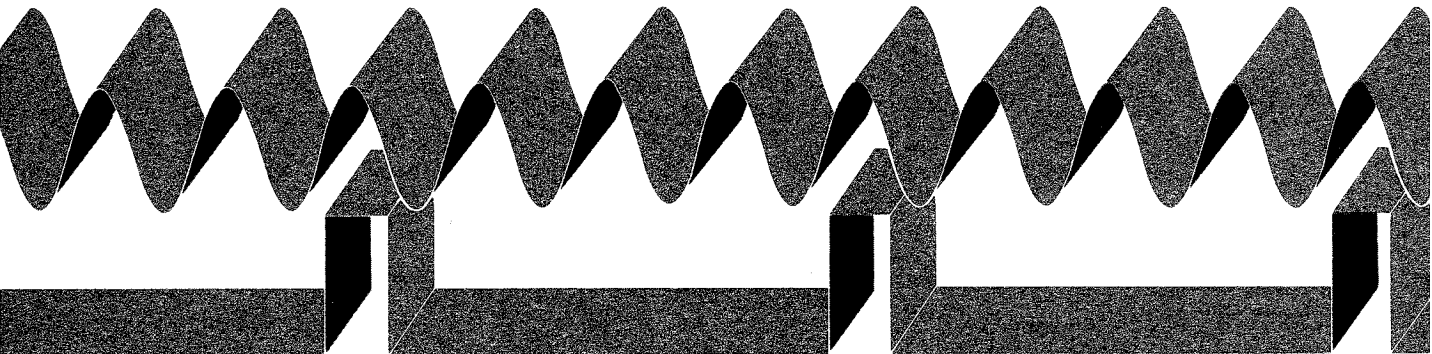
APPENDIX E

DAILY PHASE VALUES AND TIME DIFFERENCES SERIES 4

U.S. NAVAL OBSERVATORY
WASHINGTON, D.C. 20390

11 SEPTEMBER 1975

DAILY PHASE VALUES AND TIME DIFFERENCES SERIES 4

NO. 449

REFERENCES: (A) TIME SERVICE INFORMATION LETTER OF 15 AUGUST 1973
           (B) TIME SERVICE ANNOUNCEMENT, SERIES 9, NO. 36 (LORAN-C)
           (C) DAILY PHASE VALUES AND TIME DIFFERENCES, SERIES 4, NO. 389 (LORAN-D)
           (D) DAILY PHASE VALUES AND TIME DIFFERENCES, SERIES 4, NO. 195 (TV)

THE TABLE GIVES: UTC(USNO MC) - TRANSMITTING STATION   UNIT = ONE MICROSECOND

*MEASURED BY USNO TIME REFERENCE STATIONS AND OTHER MONITORING ACTIVITIES WHICH ARE
WITHIN GROUND WAVE RANGE. THESE VALUES ARE CORRECTED TO REFER TO USNO MASTER CLOCK.
**COMPUTED FROM DIFFERENTIAL PHASE DATA PROVIDED BY US COAST GUARD STATIONS AND OTHER
MONITORING ACTIVITIES. THESE VALUES ARE CORRECTED TO REFER TO USNO MASTER CLOCK.

FREQUENCY KHZ (UTC)		LORAN-C* 9970 NORTHWEST PACIFIC 100	LORAN-C* 4990 CENTRAL PACIFIC 100	LORAN-C 9930 EAST COAST U.S.A. 100	LORAN-C** 7970 NORWEGIAN SEA 100	LORAN-C** 7990 MEDITERRANEAN SEA 100	LORAN-C 7930 NORTH ATLANTIC 100
	MJD						
AUG. 27	42651	1.1	2.9	1.82	1.9	1.3	1.6
28	42652	1.1	2.9	1.84	1.8	1.2	1.6
29	42653	1.0	2.9	1.88	1.9	1.3	1.5
30	42654	1.2	2.9	1.91	2.0	1.4	1.4
31	42655	1.3	2.9	1.91	2.0	1.5	1.5
SEP. 1	42656	1.3	3.0	1.93	2.0	1.6	1.5
2	42657	1.4	3.0	1.91	2.0	1.6	1.6
3	42658	1.4	3.1	1.90	2.1	1.6	1.6
4	42659	1.5	3.1	1.90	2.2	1.7	1.6
5	42660	1.6	3.2	1.89	2.1	1.7	1.6
6	42661	1.6	3.1	1.90	2.1	1.6	1.7
7	42662	1.7	3.2	1.87	2.1	1.5	1.5
8	42663	1.6	3.3	1.78	2.1	1.6	1.5
9	42664	1.9	3.2	1.76	2.1	-	1.6
10	42665	1.9	3.3	1.75	2.0	-	1.5

FREQUENCY KHZ (UTC)		LORAN-C* 5930 NORTH PACIFIC 100	LORAN-D 4930 WEST COAST U.S.A. 100	6 OMEGA ND 10.2 6,000+	7 OMEGA ND 13.1 6,000+	5 OMEGA ND 13.6 6,000+
	MJD					
AUG. 27	42651	-4.8	9.3	443	444	445
28	42652	-4.7	9.5	443	444	445
29	42653	-4.7	9.6	443	444	445
30	42654	-4.7	-	443	444	445
31	42655	-4.7	-	442	443	445
SEP. 1	42656	-4.7	-	442	445	445
2	42657	-4.7	10.1	-	-	-
3	42658	-4.7	10.2	-	-	-
4	42659	-4.7	10.4	-	-	-
5	42660	-4.7	10.5	-	-	-
6	42661	-4.7	-	-	-	-
7	42662	-4.7	-	-	-	-
8	42663	-4.7	11.0	-	-	-
9	42664	-	11.2	-	-	-
10	42665	-	11.4	-	-	-

FREQUENCY KHZ (UTC)		1 OMEGA T 13.6 11,000+	4 GBR 16.0 19,000+	2 NAA 17.8 3,000+	3 NLK 18.6 12,000+	8 NBA 24.0 10,000+	WASHINGTON, DC WTTG *** CHANNEL 5 EMITTED
	MJD						
SEP. 4	42659	647	516	209	586	820	-1.40
5	42660	647	516	209	589(NOTE 1)	820	-1.48
6	42661	647	515	210	588	820	-1.52
7	42662	647	515	210	588	820	-1.48
8	42663	647	515	209	588	820	-1.45
9	42664	647	514	208	588	820	-1.45
10	42665	647	513	208	588	820	-1.33

*** CHANNEL 5 (WTTG) READINGS.
   THE VALUES GIVEN REPRESENT AN AVERAGE OF 30 MEASUREMENTS DURING THE 30 SECOND
   INTERVAL BEFORE 17H 10M 43S UT. IF THESE TOAS HAPPEN TO FALL INTO A NON-
   SYNCHRONIZED PROGRAM, THE 30 TOAS BEFORE 18H 10M 43S HAVE BEEN USED. A THIRD
   MEASUREMENT, BEFORE 16H 10M 43S IS ALSO AVAILABLE ON REQUEST.

NATIONAL TELEVISION NETWORKS

		NBC	NBC	CBS	CBS	ABC	ABC
		19:25:00 UT	19:31:00 UT	19:26:00 UT	19:32:00 UT	19:27:00 UT	19:33:00 UT
	MJD						
SEP. 4	42659	13,981.8	6,959.3	20,704.1	13,681.4	1,966.5	28,310.7
5	42660	30,288.0	23,265.6	3,597.3	29,941.3	18,266.7	11,244.1
6	42661	13,227.7	6,205.2	19,858.2	12,835.5	24,899.2	17,733.2
7	46662	14,824.9	7,814.2	2,751.4	29,095.4	6,770.1	32,971.1
8	42663	12,474.5	5,452.1	19,010.7	11,988.0	433.0	26,799.4
9	42664	28,781.0	21,758.6	1,903.6	28,247.6	16,733.0	9,710.4
10	42665	11,721.0	4,698.4	18,163.3	11,140.6	33,032.9	26,010.4

NOTES: (1) NLK   4 SEP. AFTER MAINTENANCE PERIOD   STEP ABOUT PLUS 3

(2) NAVY STATIONS OFF-AIR TIMES:
       NBA   5 SEP.   0827 TO 0829 UT
             6 SEP.   2033 TO 2034 UT
       NAA   9 SEP.   1751 TO 1800 UT

   NBA WAS UNSTABLE 4 SEP. ABOUT 1820 TO 1830 UT.
   NAA'S WEEKLY MAINTENANCE PERIOD WAS ON 8 SEP. INSTEAD OF 5 SEP.

(3) OMEGA STATION OFF-AIR TIME:
       TRINIDAD   3 SEP.   0531 TO 0533 UT

(4) (9930-Z) EAST COAST LORAN-C SLAVE DANA, INDIANA WAS UNSTABLE 4 SEP. 0130 TO
    0214 UT.

(5) (9930-X, 7930-Z) EAST COAST AND NORTH ATLANTIC LORAN-C SLAVE CAPE RACE,
    NEWFOUNDLAND WAS OFF THE AIR/UNSTABLE FOR PERIODS BETWEEN THE FOLLOWING TIMES:
       5 SEP.   1030 AND 1848 UT
       6 SEP.   0958 AND 1923 UT
       7 SEP.   1200 AND 1903 UT
       8 SEP.   0946 AND 1941 UT
       9 SEP.   1007 AND 1937 UT.

(6) (9930-Y) EAST COAST LORAN-C SLAVE NANTUCKET ISLAND, MASSACHUSETTS WAS OFF THE
    AIR 6 SEP. 1401 TO 1558 UT.

(7) (4990-Y) CENTRAL PACIFIC LORAN-C SLAVE KURE, MIDWAY ISLANDS WAS/IS SCHEDULED
    TO BE OFF THE AIR 8 SEP. 1700 UT TO 9 SEP. 0100 UT AND 12 SEP. 1900 UT TO
    13 SEP. 0100 UT.

(8) (7990-M) MEDITERRANEAN SEA LORAN-C MASTER CATANZARO (SIMERI CRICHI), ITALY WAS
    SCHEDULED TO BE OFF THE AIR 10 SEP. 0700 TO 0900 UT.

(9) (9970-M) NORTHWEST PACIFIC LORAN-C MASTER IWO JIMA IS SCHEDULED TO BE OFF THE
    AIR 11 SEP. 2000 TO 2100 UT.

(10) (4990-M) CENTRAL PACIFIC LORAN-C MASTER JOHNSTON ISLAND IS SCHEDULED TO BE OFF
     THE AIR 12 SEP. 2300 UT TO 13 SEP. 0100 UT.

(11) (4990) CENTRAL PACIFIC LORAN-C CHAIN IS SCHEDULED TO BE ADVANCED 3.0
     MICROSECONDS 20 SEP. AT 2000 UT.

(12) (4930) WEST COAST U.S.A. LORAN-D WAS INCREASED IN FREQUENCY BY APPROXIMATELY
     2.5 PARTS IN TEN TO THE MINUS TWELVE ON 10 SEP.

APPENDIX F
DERIVATION OF FRACTIONAL
FREQUENCY DEVIATION EQUATION

Starting with the basic definition of frequency

$$f = \frac{1}{\tau} = \tau^{-1}$$

where:

$f =$ frequency, Hz

$\tau =$ period, s

Differentiating:

$$df = -\tau^{-2} d\tau = -\frac{d\tau}{\tau^2}$$

$$df = -\frac{d\tau}{\tau} f$$

$$\frac{df}{f} = -\frac{d\tau}{\tau}$$

from which we can, for small changes, write the approximation:

$$\frac{\Delta f}{f} = -\frac{\Delta \tau}{\tau}$$

where

$\frac{\Delta f}{f} =$ fractional frequency deviation (dimensionless)

$\Delta \tau =$ change in time accumulated over the measurement time, τ.

Also since time can be measured from an accumulation of phase of a reference oscillator:

$$\frac{\Delta \tau}{\tau} = \frac{\Delta \phi}{\phi}$$

where $\Delta \phi =$ change in phase over the total accumulated phase, ϕ, due to the reference frequency.

Which leads to the final approximation

$$\frac{\Delta f}{f} = -\frac{\Delta \tau}{\tau} = -\frac{\Delta \phi}{\phi}$$

APPENDIX G

BIBLIOGRAPHY

GENERAL

(1) Allan, D.W. et al., "Precision and Accuracy of Remote Synchronization via Network Television Broadcasts, Loran-C, and Portable Clocks". Metrologia, Vol. 8 No. 2 pp. 64-72, 1972.

(2) Baugh, R.A. and Cutler, L.S., "Precision Frequency Sources", The Microwave Journal, pp. 43-56, June 1970.

(3) Begley, W.W. and Shapiro, A.H., "Aspects of Precision Timing Systems", The Aerospace Corporation, October 1969.

(4) Blair, B.E. (Ed.) Time and Frequency: Theory and Fundamentals, NBS Monograph 140, USGPO, May 1974.

(5) Bureau International de l'Heure (BIH) Annual Report 1972, BIH, 1973.

(6) Jespersen, J.L., Blair, B.E., and Gatterer, L.E., "Characterization and Concepts of Time-Frequency Dissemination", IEEE Proceedings, Vol. 60, No. 5, pp. 502-521, May 1972.

(7) Jespersen, J.L. and Fey, L., "Time Telling Techniques", IEEE Spectrum, pp. 51-58, May 1972.

(8) Operating Procedures for PTTI Equipments, U.S. Naval Observatory Time Service Division, June 1973.

(9) Putkovich, K., "Automated Timekeeping", IEEE Transactions on Instrumentation and Measurement. Vol. 1M-21, No. 4, November 1972.

(10) Winkler, G.M.R., "Path Delay, Its Variations and Some Implications for the Field Use of Precise Frequency Standards", IEEE Proceedings, Vol. 60, No. 5, pp. 522-529, May 1972.

LORAN-C

(11) Day, Richard A., Jr., "Use of Loran-C Navigational System as a Frequency Reference", Signal, pp. 26-30, November 1973.

(12) Hefley, C. The Development of Loran-C Navigation and Timing, NBS Monograph 129, USGPO, October 1972.

(13) Loran-C Manual, Austron, Inc., March 1974.

(14) Potts, C.E., and Wieder, B., "Precise Time and Frequency Dissemination via the Loran-C System". IEEE Proceedings, Vol. 60, No. 5, pp. 530-539, May 1972.

(15) Shapiro, L. Dennis, "Time Synchronization from Loran-C", IEEE Spectrum, Vol. 5 No. 8, pp. 46-55, August 1968.

OMEGA

(16) Swanson, E.R. and Kugel, C.P., "VLF Timing: Conventional and Modern Techniques Including Omega", IEEE Proceedings, Vol. 60, No. 5, pp. 540-551, May 1972.

TELEVISION

(17) Allan, D.W., Machlan, H.E., and Marshall, J., "Time Transfer Using Nearly Simultaneous Reception Times of a Common Transmission", Proceedings of 26th Annual Symposium on Frequency Control, pp. 309-316, Electronics Industries Association, Washington, D.C. 1972.

(18) Lavanceau, J.D., Time Measurements via Television, USNO, Washington, D.C., November 1972.

(19) Lavanceau, J.D., and Carroll, D., "Real Time Synchronization via Passive Television Transmission". Proceedings 3rd Annual Precise Time and Time Interval (PTTI) Strat. Plan. Mtg. (November 16-18, 1971), USNO, Washington, D.C., pp. 331-366, 1972.

(20) Leschiutta, S., "Long Term Accuracy of Time Comparisons via TV Signal Along Radio Relay Links", IEEE Transactions on Instrumentation and Measurement. Vol. 1M-22, No. 1, pp. 84-87, March 1973.

(21) Tolman, J. et al., "Microsecond Clock Comparison by Means of TV Synchronization Pulses". IEEE Transactions on Instrumentation and Measurement. Vol. 1M-16, No. 3, pp. 247-254, September 1967.

SATELLITE

(22) Easton, R.L., "The Role of Time/Frequency in Navy Navigation Satellites", IEEE Proceedings, Vol. 60, No. 5, pp. 557-563, May 1972.

(23) Ehrlich, E., "The Role of Time/Frequency in Satellite Position Determination Systems", IEEE Proceedings, Vol. 60, No. 5, pp. 564-571, May 1972.

(24) Jespersen, J.L. et al., "Satellite VHF Transponder Time Synchronization", IEEE Proceedings, Vol. 56, No. 7, pp. 1202-1206, July 1968.

(25) Markowitz, W. et al., "Clock Synchronization via Relay II Satellite", IEEE Transactions on Instrumentation and Measurement". Vol. 1M-15, No. 4, pp. 177-184, December 1966.

(26) Steele, J. McA., Markowitz, W. and Lidbach, C.A., "Telstar Time Synchronization", IEEE Transactions on Instrumentation and Measurement. Vol. No. pp. 164-170, December 1964.

(27) Higa, W.H., "Time Synchronization via Lunar Radar", IEEE Proceedings, Vol. 60, No. 5, pp. 552-557, May 1972.

(28) Phillips, D.H., Phillips, R.E., and O'Neill, J.J., "Time and Frequency Transfer via Microwave Link", IEEE Transactions on Instrumentation and Measurement, Vol. 1M-20, No. 1, pp. 23-28, February 1971.

(29) Sanders, W.R. et al., "A Meteor Burst Clock Synchronization Experiment". IEEE Transactions on Instrumentation and Measurement. Vol. 1M-15, No. 4, pp. 184-189, December 1966.

ACKNOWLEDGEMENTS